MAX-PLANCK-INSTITUT FÜR QUANTENOPTIK

VUV GENERATION BY FREQUENCY MIXING

D.J. Brink and D. Proch

M P Q 65 October 1982

MPQ-Report
65

Max-Planck-Institut für Quantenoptik
8046 GARCHING bei MÜNCHEN, Bundesrepublik Deutschland

MAX-PLANCK-INSTITUT FÜR QUANTENOPTIK

VUV GENERATION BY FREQUENCY MIXING

D.J. Brink and D. Proch

M P Q 65 October 1982

VUV GENERATION BY FREQUENCY MIXING

D. J. Brink and D. Proch

V U V Generation
by Frequency Mixing

D.J. Brink and D. Proch

Abstract

This report documents the result of an extensive screening of recent literature that describes the use of nonlinear optical phenomena in gases or vapours for the generation of coherent short wavelength radiation.

An introductory chapter that briefly recapitulates the theoretical framework of nonlinear optical processes is followed by a compilation of recent experimental results. The purpose is to establish a scale on which the virtues and shortcomings of various resonant and nonresonant mixing schemes can be compared.

Contents

1. General theoretical background

If a number of electromagnetic waves, frequencies ω_1, ω_2 ...., travel through a nonlinear optical medium new waves with frequencies:

$$\omega_j = \omega_1 \pm \omega_2 \pm \omega_3 \pm \cdots$$

will be generated.

The growth of a particular frequency component can be obtained from the Maxwell equations for a plane wave propagating in the z-direction /1/:

$$\frac{d\tilde{E}_j}{dz} = \frac{i\omega_j}{2cn_j} \mathcal{P}_j^{NL} \exp(-ik_j z) \qquad (1)$$

where $\tilde{E}_j$ is the slowly varying (complex) amplitude, n_j and k_j are the index of refraction and wavenumber at ω_j respectively. The non-linear polarization is given by /1/:

$$\mathcal{P}_j^{NL} = N \Sigma K(-\omega_j; \omega_1 \omega_2 \cdots) \chi^{(j)}(-\omega_j; \omega_1 \omega_2 \cdots) E_1 E_2 \cdots \qquad (2)$$

where the sum is taken over all combinations of ω_1, ω_2, ... which yield ω_j. The higher order susceptibilities ($\chi^{(j)}$) get progressively smaller. N is the number density and K is a constant.

In solids frequency doubling and 3-wave sum and difference generation leads to efficient production (1 to 30 % conversion) of wavelengths longer than ~220 nm. At shorter wavelengths gaseous media are generally employed. Here the first non-zero susceptibility is normally $\chi^{(3)}$ so that 4-wave mixing is the most commonly employed frequency up-conversion technique.

For the sake of simplicity the specific case of frequency tripling will be considered. Here equation (2) becomes /2/:

$$P_3^{NL}(\omega) = \frac{N}{4}\left[3\chi_T^{(3)}(\omega)E_3E_1^{*}E_1^{*} + \chi_S^{(3)}(\omega)E_1E_1^{*}E_1 + \chi_S^{(3)}(\omega,3\omega)E_1E_3E_3^{*}\right] \qquad (3a)$$

and

$$P_3^{NL}(3\omega) = \frac{N}{4}\left[\chi_T^{(3)}(3\omega)E_1E_1E_1 + \chi_S^{(3)}(3\omega)E_3E_3E_3^{*} + \chi_S^{(3)}(3\omega,\omega)E_3E_1E_1^{*}\right] \qquad (3b)$$

The actual frequency tripling is due to the first term of (3b) ($\chi_T^{(3)}(3\omega)$) only. The other terms are only of importance when saturation effects are considered. In (3a) the first term describes some backwards transfer of 3ω to ω. The real parts of $\chi_S^{(3)}$ (single and mixed frequency terms) describe intensity dependent changes of refractive index (2^{nd}-order Kerr effect). The imaginary parts of $\chi_S^{(3)}(\omega)$ and $\chi_S^{(3)}(3\omega)$ are responsible for two-photon absorption at ω and 3ω while the imaginary parts of the

mixed frequency terms ($\chi_S^{(3)}(\omega,3\omega) = \chi_S^{(3)}(3\omega,\omega)$) give rise to Raman-type gain or loss.

If all saturation and pump-depletion effects are neglected, equation (1) can be integrated directly to yield an expression for power conversion efficiency /1, 3/:

$$\eta = \left(\frac{P_3}{P_1}\right) = \frac{3\,g\,k_{01}^2}{n_3}\,\pi^2 N^2 |\chi_T^{(3)}|^2 L^2 \left(\frac{P_1}{A}\right)^2 \mathrm{sinc}^2\left(\frac{\Delta k L}{2}\right) \qquad (4a)$$

For general 4-wave mixing one obtains similarly:

$$\eta = \frac{P_4}{P_1+P_2+P_3} = g\pi^2 \frac{n_2 n_3}{n_1 n_4^2} \frac{k_{04}^2 k_{02} k_{03}}{k' k_{01}} N^2 |\chi_T^{(3)}|^2 L^2 (xy) \left(\frac{P_1}{A}\right)^2 \mathrm{sinc}^2\left(\frac{\Delta k L}{2}\right) \qquad (4b)$$

where
$g = 1.755 \times 10^{-5}$ for $\omega_1 = \omega_2 = \omega_3$
$= 1.580 \times 10^{-4}$ for any two ω_i degenerate
$= 6.318 \times 10^{-4}$ for $\omega_1 \neq \omega_2 \neq \omega_3$

$k' = k_1 \pm k_2 \pm k_3$

$\Delta k = k_4 - k'$

k_{oj} = vacuum wavenumber ω_j/c

L,A = interaction length and cross-section area.

Most of the pertinent features of 4-wave mixing can be inferred from equations (4).

2. General optimization considerations and limitations

2.1 Influence of power and conversion length

From (4) it is evident that high power densities are essential for good conversion. Power density can be increased by focusing. However, once the high power-density region lies entirely inside the non-linear medium little can be gained by going to an even tighter focus, because harder focusing reduces the effective interaction length L. In practice $L \simeq 2b$, with $b = k_j w_o^2$ = Rayleigh length.

If a focused Gaussian beam is used instead of a plane wave, equation (4b) becomes /3/:

$$P_4 = \frac{g k_{04}^2 k_{01} k_{02} k_{03}}{k'} \left(\frac{n_1 n_2 n_3}{n_4^2}\right) N^2 |\chi_T^{(3)}|^2 P_1 P_2 P_3 \, F\left(b\Delta k, \frac{b}{L_c}, \frac{f}{L_c}, \frac{k''}{k'}\right) \qquad (5a)$$

where L_c = cell length

f gives the location of the beam waist (f = 0.5 L_c is centre)

$k'' = k_1 + k_2 + k_3$.

For frequency tripling the expression simplifies to:

$$\eta = \left(\frac{P_4}{P_1}\right) = 3 g k_{01}^4 \frac{n_1^2}{n_4^2} N^2 |\chi_T^{(3)}|^2 P_1^2 F \qquad (5b)$$

The function F is determined by the focusing conditions.

For very loose focusing:

$$\lim_{\frac{b}{L_c}\to\infty} F = \frac{4L^2}{b^2} \operatorname{sinc}^2\left(\frac{\Delta k L}{2}\right)$$

and we get the plane-wave case again. For tight focusing and sum frequency generation:

$$\lim_{\frac{b}{L_c}\to 0} F_{sum}(b\Delta k, 0, 0.5, 1) = \pi^2 (\Delta k b)^2 e^{(b\Delta k)} \quad \text{for } \Delta k < 0 \qquad (6a)$$

$$= 0 \quad \text{for } \Delta k \geq 0$$

This function is optimized at a value of 5.34 for $b\Delta k = -2$.

In the case of tight focusing and difference frequency generation ($\omega_4 = \omega_1 + \omega_2 - \omega_3$) one obtains:

$$\lim_{\frac{b}{L_c}\to 0} F_{dif}(b\Delta k, 0, 0.5, 1) = \pi^2 e^{-b|\Delta k|} \qquad (6b)$$

In systems which show saturation effects at fairly low power densities it is usual to use loose focusing and to make the cell as long as practically possible. Power conversion is then given by equation (4).

Systems which only saturate at very high intensities are usually employed with tight focusing arrangements to get $b << L_c$ and thereby the best conversion. Equations (5) and (6) should be used in this case.

2.2 Phase matching

Optimum conversion can only be obtained if the phase velocities of the driving polarization and the generated wave are equal. If this is not the case constructive-destructive interference will cause the signal to oscillate between a maximum value and zero over the interaction length. In the plane-wave case phase matching is achieved by simply making $\Delta k = 0$. This can be achieved by working near to the short wavelength side of a resonance (for 3ω) where a negative dispersion is obtained. The negative Δk value so obtained can then be compensated by adding a normal positively dispersing component.

In focusing a Gaussian beam an additional phase slip develops between the driving polarization and the generated wave. This can be seen by referring to the standard expression for a Gaussian beam /4/:

$$E(r,z,t) = E_0 \frac{w_0}{w} e^{i(kz-\phi)} e^{-i\omega t} e^{w^2/r^2}; \qquad \phi = \tan^{-1}\left(\frac{z}{b}\right) \tag{7a}$$

According to equation (2) the driving polarization is then:

$$P_3^{NL}(3\omega) \propto E(r,z,t)^3 = E_0^3 \left(\frac{w_0}{w}\right)^3 e^{i(3kz-3\phi)} e^{-i3\omega t} e^{w_3^2/r^2} \tag{7b}$$

Since the generated wave has the same b value as the fundamental it follows the phase as in (7a). One sees that a phase difference of $2\tan^{-1}(Z/b)$ develops between

this and $P_3^{NL}(3\omega)$. This additional phase slip can be compensated by using a gas mixture with a net negative dispersion. The magnitude of the negative dispersion required is given by the behaviour of the function F in (5).

For sum generation under tight focusing conditions F peaks for $\Delta k = -2/b$. The tighter the focus, the more negative the net dispersion must therefore be.

For difference generation ($\omega_4 = \omega_1 + \omega_2 - \omega_3$) f is optimized for $b\Delta k = 0$. In this case no additional phase slip is introduced by focusing, since:

$$P_3^{NL}(\omega_1+\omega_2-\omega_3) \propto E_1 E_2 E_3^* \propto e^{i[(k_1+k_2-k_3)z - \phi - \phi + \phi]}$$

and conversion is optimized by always focusing as tightly as possible.

2.3 Particle density

Conversion efficiency depends on the square of the particle density. In a single component mixture the optimum yield is obtained at a trade-off between phase matching (function F) and a high $N^2|\chi|^2$ value, a well defined optimum therefore exists for N.

If a multi-component mixture is employed the density term in (4) and (5) should be changed to:

$$N^2 |\chi|^2 \longrightarrow |\sum N_i \chi_i^{(3)}|^2 \qquad (8)$$

where the sum is taken over all ingredients having large third-order susceptibilities. Here phase matching is effectively uncoupled from density and conversion is optimized by simply maximizing the density of all ingredients with large $\chi^{(3)}$ values . However, even for non-resonant systems, the particle density (and interaction length) is limited by absorption of the generated wavelength into the wing of the resonance line providing the negative dispersion.

Increasing density (especially of the negatively dispersing component) leads to increased dispersion which finally puts a limit on the bandwidth over which phase matching can be maintained. When the line width becomes comparable to the acceptance bandwidth of the system the yield can be expected to drop. Narrow linewidth sources are therefore to a certain extent a prerequisite for high yields /5/.

The optimum mixing ratio follows from the phase-matching condition:

$$\Delta k = k_3 - 3k_1 = \frac{6\pi}{\lambda_1}(n_3 - n_1) = -\frac{q}{b} \qquad (9a)$$

where q = 2 for tight focusing

= 4 for loose focusing

For a two component system $N = N_A + N_B$, with a mixing ratio of $N_B/N_A = R$, this becomes:

$$\Delta k = \frac{6\pi}{\lambda_1}(\alpha + \beta R)\frac{N}{1+R} = -\frac{q}{b} \qquad (9b)$$

where $\alpha N_A = (n_3 - n_1)_A$ and $\beta N_B = (n_3 - n_1)_B$.

The optimum mixing ratio is then:

$$R = \frac{-6\pi b N\alpha - \lambda_1 q}{6\pi b N\beta + \lambda_1 q} \qquad (10a)$$

which for loose focusing (or just large enough b) reduces to:

$$R = -\frac{\alpha}{\beta} \qquad (10b)$$

In many systems the negatively dispersing component has the dominant $\chi^{(3)}$ value. In this case we can substitute N from (9b) into (5) without the (1+R) factor:

$$\eta = q_3^2\, g\, k_{01}^2 \frac{n_1^2}{n_3^2} |\chi_{TA}^{(3)}|^2 P_1^2 \frac{F_{max}}{b^2(\alpha+\beta R)^2} \qquad (11a)$$

Note that the $1/b^2$ dependence is only apparent, since b and R are related.

2.4 The Susceptibility

A good yield obviously requires a large non-linear susceptibility. Unlike the linear susceptibility both real and imaginary parts of $\chi^{(3)}_T$ contribute in the same way. Expressions for the susceptibilities in (3) are /2/:

$$\chi^{(3)}_T(3\omega) = \hbar^{-3} \sum_{a,b,c} \frac{\mu}{(\omega_{ag}-\omega)(\omega_{bg}-2\omega)(\omega_{cg}-3\omega)} \qquad (12a)$$

$$\chi^{(3)}_S(\omega) = \hbar^{-3} \sum_{a,b,c} \frac{\mu}{(\omega_{ag}-\omega)(\omega_{bg}-2\omega)(\omega_{cg}-\omega)} \qquad (12b)$$

$$\chi^{(3)}_S(3\omega,\omega) = \hbar^{-3} \sum_{a,b,c} \frac{\mu}{(\omega_{ag}-3\omega)(\omega_{bg}-2\omega)(\omega_{cg}-3\omega)} \qquad (12c)$$

where $\mu = \mu_{ga}\,\mu_{ab}\,\mu_{bc}\,\mu_{cg}$, the dipole matrix elements for the various transitions outlined in the diagram:

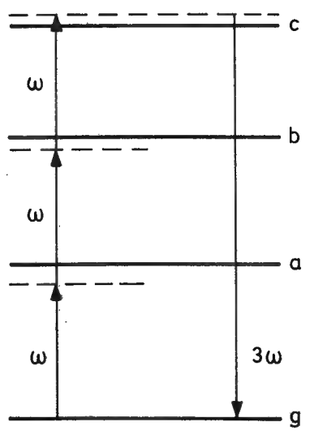

Fig. 1

and $\omega_{ij} = \Omega_{ij} - i\,\Gamma_{ij}$ with Γ_{ij} related to the line width of the transition $i \to j$ and Ω_{ij} the transition frequency.

Equations (12) show that the susceptibilities can be greatly enhanced by working near atomic resonances. Such a procedure will, however, also affect the $\chi^{(3)}_s$ terms and one can expect that saturation effects will be more prominent in resonantly enhanced mixing than for the non-resonant processes. A further important difference between resonant and non-resonant mixing is that in the former case ($\Omega_{ij}-\omega = 0$) the imaginary parts of $\chi^{(3)}_s$ dominate, i.e. absorption effects will limit the conversion whereas with non-resonant processes the real parts of $\chi^{(3)}_s$, i.e. refractive index changes, dominate.

The most important absorption effects are pump depletion due to two- or multi-photon absorption, depletion of the groundstate population (which has the large $\chi^{(3)}_T$ values) and refractive index changes due to the buildup of excited-state populations. As an example, the cross section for two-photon absorption is intensity dependent:

$$\sigma^{(2)}(2\omega) = 2\omega\left(\frac{2\pi}{c}\right)^2 I\{\chi^{(3)}_s(\omega)\}\left(\frac{P_i}{A}\right)$$

The result is that one usually obtains an optimum intensity for best conversion, this intensity value is often quite

low. The conversion formulae given by Vidal /2/ for optically thick media (strong single photon absorption at ω or 3ω) also show that saturation can be expected at quite low intensities. Other limitations encountered with resonantly enhanced mixing are power broadening and high frequency Stark-shifting of the resonances involved.

When working with non-resonant systems the situation is quite different. Intensity induced refractive-index changes, which lead to a break in the phase-matching condition, usually limits conversion long before any depletion effects are noticeable. These refractive-index changes can normally not be compensated by the gas dispersion, because it is not constant across the beam profile. Limiting power densities are, however, normally several orders of magnitude larger than those obtained with resonant mixing.

The power dependent refractive index changes (2^{nd}-order Kerr effect) can be included in the conversion formula (11a) /6/:

$$\eta = \frac{\bar{\pi}^2 q^2 g}{3 n_3^2} |\chi_T|^2 \left(\frac{P_i}{A}\right)^2 \frac{F_{max}}{(\alpha + \beta R + \gamma (\frac{P_i}{A}))^2} \qquad (11b)$$

where $\gamma = 0.079\ [\chi_s^{(3)}(3\omega,\omega) - 1/2\ \chi_s^{(3)}(\omega)]$ and $A = \pi w_o^2 = \pi b/(k_{o1} n_1)$. At very high power densities we therefore obtain a conversion which is independent of all

experimental parameters:

$$\eta_{max} = 0.11 \left[\frac{\chi_T^{(3)}(3\omega)}{\chi_s^{(3)}(3\omega,\omega) - \frac{1}{2}\chi_s^{(3)}(\omega)}\right]^2 \qquad (11c)$$

This value of η is a useful figure of merit for the non-linear medium employed.

A further disadvantage of working too close to a resonance is the increased dispersion which reduces the acceptance bandwidth of the system and the increased absorption of the generated wavelength.

3. Summary of recent experimental results

3.1 Non-resonant systems

Non-resonant systems offer the possibility of wide tunability and good conversion if adequate pump power is available. Saturation effects (mainly second-order Kerr effect and self focusing) only start playing a role at intensities in excess of 10^{10} to 10^{11} W cm^{-2} for metal vapours /7/ and $\gtrsim 10^{12}$ W cm^{-2} for most noble gases /6/.

Metal-vapour systems have resonance lines at longer wavelengths and are therefore mostly used in the nearer UV ($\lambda > 200$ nm). The large non-linear susceptibilities of metal vapours also make them attractive at somewhat

shorter wavelengths. Here auto-ionizing levels lying well above the ionization limit can be employed to furnish the required negative dispersion and large $\chi^{(3)}$-values /8/.

The lower saturation limits of metal vapours make the use of a fairly loose focusing geometry necessary. Interaction length is therefore made as long as practically possible (typically 30 to 40 cm). Vapour density and total gas pressure are limited by "fogging", i.e. vapour condensation in the cold buffer-gas atmosphere at the ends of the cell, to about 6 mbar and 1200 mbar respectively /7, 9/.

In the metal-vapour case good spatial properties of the pump laser beam (single mode operation) and a high degree of temperature uniformity (better than $\sim 0.5^{o}$ C) are essential to maintain phase matching over an extended length /10/.

With high pump powers (> 200 MW) conversion efficiencies of up to 3 % and 10 % were obtained for frequency tripling a mode locked Nd-YAG laser in Na and Rb vapours /7, 9/. At more moderate power levels (1 - 10 MW) conversions ranging from 10^{-7} to 10^{-4} are reported /11/.

The high saturation intensities observed in noble-gas systems make it possible to use short cells (few cm long)

with very tight focusing /12/. The maximum gas density is now limited by acceptance bandwidth and wing absorption considerations. Calculations show, for example, that the bandwidth of a Kr-Xe system (200 mbar Kr, 67 mbar Xe) used for generation of 121,6 nm radiation is less than 0.1 nm /5/. In this case tighter focusing improved the bandwidth. Narrow bandwidth pump lasers are therefore necessary for most noble-gas systems.

In Ar, Kr and Xe several wavelength intervals between 80 and 147 nm show the required negative dispersion characteristics /5/ (see Fig. 2). The latter two also provide fairly good non-linear susceptibilities in this range. Shorter wavelengths can be generated in Ne and He, but low $\chi^{(3)}$ values reduce the yields. In a recent experiment, for example, wavelengths as short as 57 nm were generated in Ar with conversions of $\sim 10^{-8}$ /13/.

The best conversion efficiencies reported to date are $\sim$ 1 % for frequency tripling 354,7 nm (3 x mode locked Nd-YAG at power > 200 MW) in a Xe-Ar-mixture. At the power levels obtainable from narrow-band tunable dye-lasers ($\sim$ 2 MW) conversions ranging from 10^{-5} to 10^{-6} are reported for the spectral region 100 - 200 nm /14, 15/.

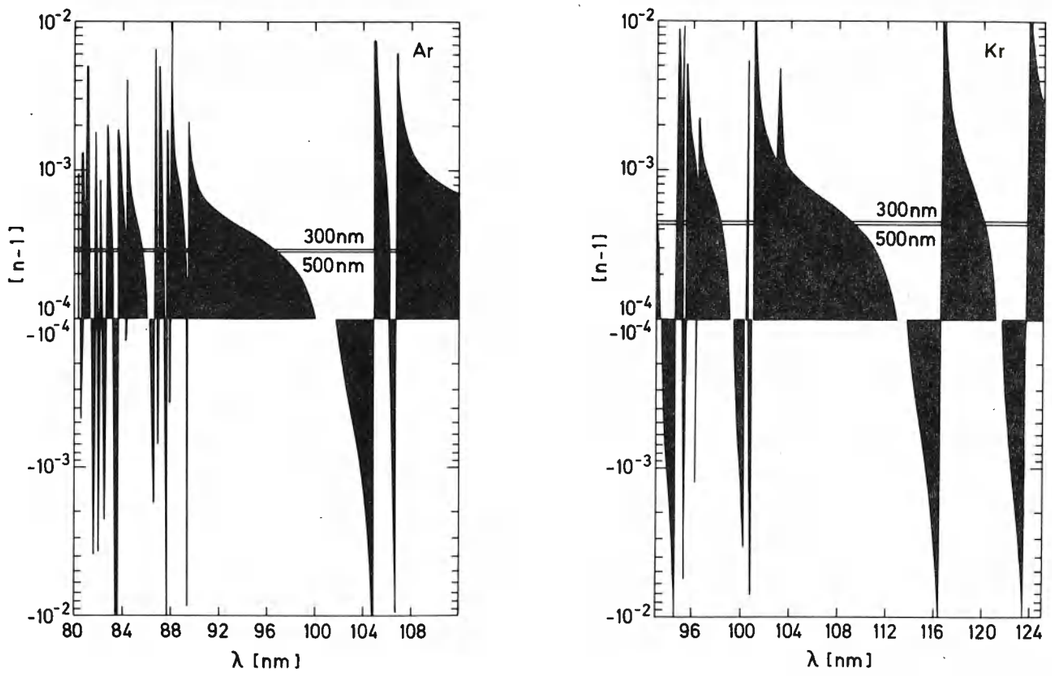

Fig. 2

3.2 Resonantly-enhanced systems

As expected on the basis of the theory outlined in section 2.4 a considerable improvement (several orders of magnitude /16/) can be obtained by employing a two-photon resonance. A further improvement can be attained if in addition a second resonance can also be utilized. This resonant enhancement is , however, only possible at relatively low power levels, where saturation effects are small. Saturation is reported at intensities of 10^7 - 10^8 W cm^{-2} for 2-photon resonances in metal vapours /17, 18/.

In resonantly enhanced systems the interaction length and particle densities are mainly limited by pump depletion and absorption of the generated wavelength.

Pumping with very high powers (∿ 250 MW) a conversion approaching 10^{-3} was obtained in Ca vapour /19/. Similar conversions were recently obtained at much lower power levels (∿ 1 MW) in Xe /20/. At even more reduced powers (∿ 30 KW) conversions of 5 x 10^{-6} were observed in Mg-vapour /21/. These examples clearly demonstrate the importance of saturation effects in resonant mixing.

Direct frequency tripling obviously allows almost no tunability. Good tunability can nevertheless be obtained by mixing the light from two different lasers ($\omega_4 = 2\omega_1 \pm \omega_2$):

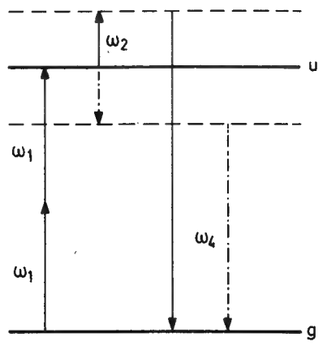

Fig. 3

Three-photon resonantly-enhanced mixing offers the possibility of very efficient frequency up-conversion of weak IR-signals (ω_s). The basic scheme is identical to that outlined in fig. 3 except that a real level now coincides with $2\omega_1 \pm \omega_2$. Power conversions $P(\omega_4)/P(\omega_s)$ of up to a factor of 10 have been reported /22/. Good tunability (in signal wavelength ω_s) can be obtained by using two pump lasers, one of which is tunable /23/:

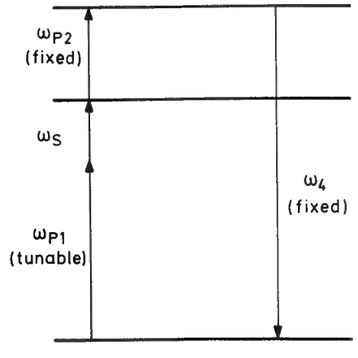

Fig. 4

This scheme also provides efficient tunable generation of IR light (at ω_s) if ω_4 is provided as input /22/.

An interesting phenomenon, which takes place only in the case of resonantly enhanced mixing, is that of phase locking. At sufficiently high intensities of all four waves involved in the mixing process, a modulation of the refractive index of the medium occurs, which causes automatic phase matching to a certain extent /24/. The power levels at which this effect occurs depend on the existing degree of phase mismatch between the four waves.

4. Other mixing processes of interest in VUV-generation

4.1 Raman-type processes

The strong Stokes field generated by stimulated Raman scattering (SRS) in many gases (especially H_2) can be used in conjunction with the pump wave in a 4-wave mixing process to generate blue-shifted anti-Stokes (AS) lines:

$$\omega_{AS}(1) = 2\,\omega_p - \omega_s$$

Once the first AS-wave is generated a whole sequence of higher-order AS-lines can be produced in the same way:

$$\omega_{AS}(n) = \omega_p + \omega_{AS}(n-1) - \omega_s$$

In H_2 a shift of 4155 cm^{-1} is obtained for each AS-order and overall efficiencies of $\sim 5 \times 10^{-4}$ are reported for a combination of 8 shifts (100 mJ; 550 nm → 50 µJ; 193 nm) /25, 26, 35/.

Since this is basically a resonantly enhanced frequency difference process:

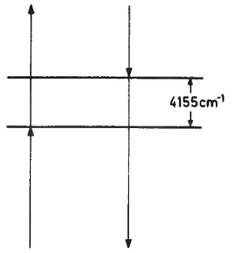

Fig. 5

no additional phase change occurs upon focusing and phase matching is obtained by slightly off-axis propagation of the generated waves /27/. Phase locking is also expected in this case /28, 36/.

Stimulated electronic Raman scattering (SERS) is a process where double resonant enhancement in metal vapours is employed to generate UV or VUV in a single AS-shift. Since electronic transitions are involved, large shifts are possible. In this case 4-wave mixing does not occur and the medium must first be pumped to produce a population inversion:

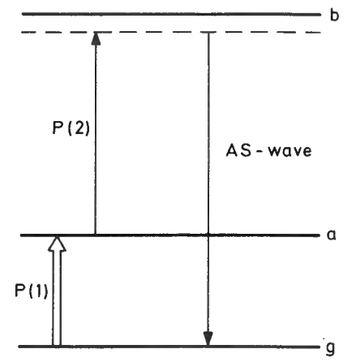

Fig. 6

The pump process usually takes the form of a selective photodissociation step. Good conversion efficiencies are for example reported for the process /29/:

$TlCl + \nu$ (26 mJ; 193 nm) → $Tl^* + Cl$

$Tl^* + \nu$ (25 mJ; 530 nm) → $Tl + \nu$ (1.8 mJ; 376 nm)

A similar process in Iodine generates VUV light at ∿ 178 nm /30/:

$NaI + \nu$ (2 mJ; 248 nm) → $Na + I^*$

$I^* + \nu$ (75 µJ; 206 nm) → $I + \nu$ (35 µJ; 178 nm)

Due to the double resonance involved the tunability is rather limited.

4.2 Higher order processes

Frequency mixing due to high-order susceptibilities ($\chi^{(n)}$; n = 5, 7, 9, ...) is generally expected to provide a substantially lower yield than lower order processes. However, the use of higher-order interactions allows larger frequency shifts in a single conversion step.

As a measure of the obtainable conversion one can compare the non-linear polarization associated with two successive orders /31/:

$$\frac{P_{(q+2)}}{P_{(q)}} = \frac{\chi^{(q+2)}}{\chi^{(q)}} \left(\frac{E}{2}\right)^2 \qquad (13)$$

At sufficiently high intensities one can therefore expect the high-order processes to become comparable or even stronger than the lower orders. In He, for example, this should happen at pump intensities exceeding $\sim$ 5 x 10^{12} W cm^{-2} for q = 3 and a pump wavelength of 266 nm (4 x Nd-YAG).

In this example saturation effects were noted for intensities $\gtrsim$ 5 x 10^{13} W cm^{-2} (12 MW pump power). At this power level a conversion of $\sim 10^{-7}$ was obtained for 5th harmonic generation (52 nm). Increasing the intensity to $\sim 10^{15}$ W cm^{-2} (300 MW pump power) improved the conversion to $\sim 10^{-5}$ /32/. As expected on the basis of

equation (13) the 3rd harmonic yield was lower by about a factor of 10 in this experiment. At the maximum pump intensity the 7th harmonic at 38 nm was also observed with a conversion efficiency of $\sim 10^{-6}$ /33/.

The optimum phase-matching conditions for high-order processes were calculated to be /33/:

$$\begin{aligned} b\Delta k &= -10.4 \quad 5^{th} \text{ order} \\ &= -14.6 \quad 7^{th} \text{ order} \end{aligned} \qquad (14)$$

In this calculation the beam waist was assumed to be on the exit window.

To date the highest order frequency mixing observed is the 9th harmonic of Nd-YAG in Na vapour. A very low conversion of $\sim 10^{-16}$ was observed /34/.

Appendix

Index of refraction in gaseous media

The refractive index of a gas can be calculated using the standard Lorenz-Lorenz formula /37/:

$$\frac{n^2-1}{n^2+2} = \frac{4}{3}\pi N \alpha \qquad \text{(A1)}$$

where N is the gas density and α is the mean polarizability (defined by the relation between polarization and electric fieldin the linear approximation: $P = N\alpha E$). The polarizability α can be expressed in terms of the resonance frequencies and oscillator strengths of the gas:

$$\alpha = \frac{e^2}{m} \sum_k \frac{f_k}{(\omega_k^2 - \omega^2) - i\,\omega_k g_k} \qquad \text{(A2)}$$

where e and m are electronic charge and mass and g_k is a damping factor related to the absorption of the medium at resonance frequency ω_k.

When working sufficiently far from resonance to ensure that $|\omega_k^2-\omega^2| >> \omega_k g_k$, α can be taken as real and absorption effects can be neglected.

For most gases expression A1 can be simplified by putting $n^2 + 2 \simeq 3$. This yields the Sellmeier formula:

$$n^2 - 1 \simeq \frac{Nr}{\pi} \sum_k \frac{f_k}{1/\lambda_k^2 - 1/\lambda^2} \qquad \text{(A3)}$$

with $r = e^2/mc^2 = 2.818 \times 10^{-13}$ cm.

In most cases this can be simplified further by putting $n^2-1 \simeq 2(n-1)$, i.e.:

$$n - 1 \simeq \frac{Nr}{2\pi} \sum_k \frac{f_k}{1/\lambda_k^2 - 1/\lambda^2} \qquad \text{(A4)}$$

The effect of continuum absorption on the refractive index can be included in a similar fashion /5/:

$$(n-1)_{cont} = \frac{N}{2\pi^2} \int_0^\infty \frac{\sigma\, d\bar{\nu}_i}{\bar{\nu}_i^2 - \bar{\nu}^2} \qquad \text{(A5)}$$

where σ is the (frequency dependent) ionization cross-section (cm^2) and $\bar{\nu}_i$ is measured in units of cm^{-1} ($1/\lambda$). In most cases σ varies sufficiently slowly to allow numerical calculation according to:

$$(n-1)_{cont} = \frac{N \Delta\lambda_i}{2\pi^2} \sum_i \frac{\sigma_i}{1 - (\lambda_i/\lambda)^2} \qquad \text{(A6)}$$

Values for ionization cross-section and oscillator strengths for the nobel gases can be found in /38-41/.

References

/1/ D.C. Hanna, M.A. Yuratich and D. Cotter
Nonlinear Optics of Free Atoms and Molecules
(Springer-Verlag, Berlin, Heidelberg, New York 1979)
pp. 17, 87, 91

/2/ C.R. Vidal
Coherent VUV sources for high resolution spectroscopy
Appl.Opt. 19, 3897-3903 (1980)

/3/ G.C. Bjorklund
Effects of Focusing on Third-Order Nonlinear Processes
in Isotropic Media
IEEE J.Quant.Electron. 11, 287-296 (1975)

/4/ H. Kogelnik and T. Li
Laser Beams and Resonators
Proc. IEEE 54, 1312-1329 (1966)

/5/ R. Mahon, T.J. McIlrath, V.P. Myerscough and D.W.Koopman
Third-harmonic Generation in Argon, Krypton, and Xenon:
Bandwidth Limitations in the Vicinity of Lyman-α.
IEEE J.Quant.Electron. 15, 444-451 (1979)

/6/ L.J. Zych and J.F. Young
Limitations of 3547 to 1182 Å Conversion Efficiency
in Xe
IEEE J.Quant.Electron. 14, 147-149 (1978)

/7/ D.M. Bloom, G.W. Bekkers, J.F. Young and S.E. Harris
Third harmonic generation in phase-matched alkali
metal vapours
Appl.Phys.Lett. 26, 687-689 (1975)

/8/ J.A. Armstrong and J.J. Wynne
Autoionizing states of Sr studied by the generation
of tunable vacuum UV radiation
Phys.Rev.Lett. 33, 1183-1185 (1974)

/9/ D.M. Bloom, J.F. Young and S.E. Harris
Mixed metal vapour phase matching for third-harmonic
generation
Appl.Phys.Lett. 27, 390-392 (1975)

/10/ H. Puell, K. Spanner, W. Falkenstein and W. Kaiser
Third-harmonic generation of mode-locked Nd-glass
laser pulses in phase-matched Rb-Xe mixtures.
Phys.Rev. A14, 2240-2257 (1976)

/11/ A.H. Kung, J.F. Young, G.C. Bjorklund and S.E.Harris
Generation of vacuum ultraviolet radiation in
phase-matched Cd vapor
Phys.Rev.Lett. 29, 985-991 (1972)

/12/ A.H. Kung, J.F. Young and S.E. Harris
Generation of 1182 Å radiation in phase-matched
mixtures of inert gases
Appl.Phys.Lett. 22, 301-302 (1973)
Appl.Phys.Lett. 28, 239 (1976)

/13/ M.H.R. Hutchinson, C.C. Ling and D.J. Bradley
Generation of coherent radiation at 570 Å by
frequency tripling
Opt. Comm. 18, 203-204 (1976)

/14/ D. Cotter
Tunable narrow-band coherent VUV source for
the Lyman-α region
Opt. Comm. 31, 397-400 (1979)

/15/ R. Hilbig and R. Wallenstein
Narrowband tunable VUV radiation generated by
non-resonant sum- and difference-frequency mixing
in Xenon and Krypton
Appl.Opt. 21, 913-917 (1982)

/16/ R.T. Hodgson, P.P. Sorokin and J.J. Wynne
Tunable coherent vacuum-ultraviolet generation in atomic vapors
Phys.Rev.Lett. 32, 343-346 (1974)

/17/ H. Puell, H. Scheingraber and C.R. Vidal
Saturation of resonant third-harmonic generation in phase-matched systems
Phys.Rev. A22, 1165-1178 (1980)

/18/ H. Scheingraber and C.R. Vidal
Near resonant third harmonic generation
Opt. Comm. 38, 75-80 (1981)

/19/ A.I. Ferguson and E.G. Arthurs
Two photon resonant third harmonic generation in calcium vapour
Phys.Lett. 58A, 298-300 (1976)

/20/ R. Hilbig and R. Wallenstein
Generation of narrowband tunable VUV radiation
Appl.Phys. B28, 202-203 (1982)

/21/ H. Scheingraber, H. Puell and C.R. Vidal
Quantitative analysis of resonant third-harmonic generation in strontium
Phys.Rev. A18, 2585-2591 (1978)

/22/ D.M. Bloom, J.T. Yardley, J.F. Young and S.E. Harris
Infrared up-conversion with resonantly two-photon pumped metal vapors
Appl.Phys.Lett. 24, 427-428 (1974)

/23/ S.A. Komarov, V.V. Krasnikov, and V.S. Solomatin
Conversion of tunable infrared radiation in alkali metal vapors
Sov.J.Quantum.Electron. 10, 1449-1450 (1981)

/24/ V.S. Butylkin, G.M. Krachik and Yu.G. Khronopulo
Contribution to the theory of resonant four-wave parametric interactions
Sov.Phys.JETP 41, 247-252 (1975)

/25/ V.Wilke and W.Schmidt
Tunable coherent radiation source covering a spectral range from 185 to 880 nm
Appl.Phys. 18, 177-181 (1979)

/26/ H. Schomburg, H.F. Döbele and B. Rückle
Tunable narrow line amplification in ArF* and anti-Stokes production around 179 nm
Appl.Phys. B28, 201 (1982)

/27/ A.N. Arbatskaya and M.M. Sushchinskii
Investigation of four-photon processes in stimulated Raman scattering (SRS)
Sov.Phys. JETP 39, 981-984 (1975)

/28/ V.S. Butylkin, V.G. Venkin, V.P. Protasov, P.S. Fisher, Yu.G. Khronopulo and M.F. Shalyaev
Effect of phase locking on the dynamics of the anti-Stokes component of stimulated Raman scattering
Sov.Phys. JETP 43, 430-435 (1977)

/29/ J.C. White and D. Henderson
Anti-Stokes Raman Laser
Appl.Phys. B28, 124 (1982)

/30/ J.C. White and D. Henderson
A 178 nm Iodine anti-Stokes Raman Laser
Appl.Phys. B28, 125 (1982)

/31/ J. Reintjes, C.Y. She and R.C. Eckardt
Generation of coherent radiation in the XUV by fifth- and seventh-order frequency conversion in rare gases
IEEE J.Quant.Electron. 14, 581-596 (1978)

/32/ J. Reintjes and C.Y. She
Comparison of fifth- and third harmonic conversion in He
Opt. Comm. 27, 469-474 (1978)

/33/ J. Reintjes
Frequency mixing in the extreme ultraviolet
Appl.Opt. 19, 3889-3896 (1980)

/34/ M.G. Grozeva, D.I. Metchkov, U.M. Mitev, L.I. Pavlov, and K.V. Stamenov
Direct ninth harmonic conversion of picosecond laser pulses
Opt.Comm. 23, 77-79 (1977)

/35/ D.J. Brink and D. Proch
Efficient tunable ultraviolet source based on stimulated Raman scattering of an excimer-pumped dye laser
Optics Letters (1982), in print

/36/ D.J. Brink and D. Proch
Angular distribution of high-order anti-Stokes stimulated Raman scattering in hydrogen
J.Opt.Soc.Am. (1982), in print

/37/ M. Born and E. Wolf
Principles of Optics - 3rd ed.
(Pergamon Press - New York 1965) pp. 85-97

/38/ G.V. Marr and J.B. West
Absolute photoionization cross-section tables for helium, neon, argon and krypton in the VUV spectral regions
Atom.Data and Nucl.Data Tables 18, 497-508 (1976)

/39/ J.B. West and J. Morton
Absolute photoionization cross-section tables for Xe in the VUV and the soft X-ray region
Atom. Data and Nucl. Data Tables 22, 107 (1978)

/40/ J. Geiger
Proc. 4th Int.Conf. VUV Radiation Physics
(Pergamon Press - New York, 1974) p. 28

/41/ J. Geiger
Energy loss spectra of Xe and Kr and their analysis by energy dependent multichannel quantum defect theory
Z. Physik A 282, 129-141 (1977)